

# Nanostructured WO<sub>3</sub> deposited by modified thermal evaporation for gas-sensing applications

A. Ponzoni\*, E. Comini, M. Ferroni, G. Sberveglieri

*SENSOR Laboratory, INFN-Dipartimento di Chimica e Fisica per l'Ingegneria e per i Materiali, Università di Brescia, via Valotti 9, 25133 Brescia, Italy*

Available online 13 June 2005

## Abstract

In this work, we present a simple method, based on a modified thermal evaporation technique, to obtain films of nanostructured WO<sub>3</sub> with high surface roughness. This method consists on sublimation from a metallic tungsten wire followed by oxidation in low vacuum conditions and reactive atmosphere ( $p_{O_2}=0.22$  mbar), with substrates heated at high temperature (600 °C). Electron microscopy (SEM, TEM) and atomic force microscopy (AFM) analysis revealed that the deposited films are composed of agglomerates with nanometric size and present high surface roughness and large effective area suitable for gas-sensing applications. Sensing measurements highlighted promising performances, particularly at the working temperature of 100 °C: high responses towards sub-ppm concentrations of NO<sub>2</sub> have been observed compared to the lower ones observed for NH<sub>3</sub> and CO. NO<sub>2</sub> tests performed with sensors based on sputtered thin films highlighted that sensors obtained by this thermal evaporation like method exhibit improved performances.

© 2005 Elsevier B.V. All rights reserved.

*Keywords:* Tungsten oxide; Thermal evaporation; Gas sensors

## 1. Introduction

Tungsten oxide is a widely studied material for the development of solid-state devices based on thin and thick films. The most successful results have been obtained in electrochromics [1,2] and gas sensor fields. Focusing on gas sensors, most of the work has been devoted to conductometric devices, that, due to their small size, low cost production, low power consumption and high compatibility with electronics signal processing are the most promising ones.

The sensing mechanism consists on chemisorption of gaseous molecules on the surface. As a consequence, electrons flow from the surface states to adsorbed molecules and vice versa depending on the gas. Oxidizing gases like NO<sub>2</sub> extract electrons from the conduction band while reducing ones like CO or NH<sub>3</sub> inject electrons.

The sensing properties of a material depend on its microstructure and on the reactivity of its surface. The latter

is enhanced by the presence of defects and active species like O<sup>-</sup>, O<sup>2-</sup>, OH<sup>-</sup>, H<sup>+</sup> [3]. About the microstructure, it is well established that polycrystalline films exhibit higher performances than amorphous ones [4]. Furthermore, a grain size comparable with the depletion region depth caused by chemisorption strongly enhances the sensitivity [5].

Several materials like SnO<sub>2</sub>, TiO<sub>2</sub>, ZnO and others have been studied for such applications [6–8]. WO<sub>3</sub> revealed to be a good candidate for detection of different gases like H<sub>2</sub>S [9,10], NH<sub>3</sub> [11] and H<sub>2</sub> [12], but most promising performances have been obtained for NO<sub>2</sub>. Different preparation methods have been used to obtain films with different properties. Screen printing has been adopted by Chung et al. to deposit WO<sub>3</sub> thick films [13].

Thin films have been prepared by sputtering method obtaining NO<sub>x</sub> sensors operating at 400 °C [14]. A detailed study of how deposition parameters affect the microstructure and the sensing performances of WO<sub>3</sub> sputtered thin films has been reported in [15]. Gas-sensing optimization has been highlighted to occur for a mean grain size value comparable with the depletion layer depth.

\* Corresponding author. Tel.: +39 030 3715707; fax: +39 030 2091271.

E-mail address: [ponzoni@tflab.ing.unibs.it](mailto:ponzoni@tflab.ing.unibs.it) (A. Ponzoni).

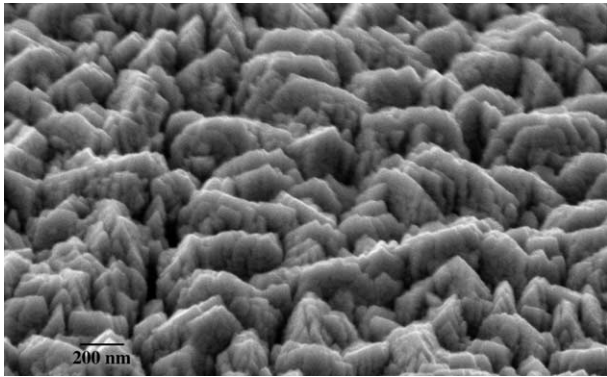


Fig. 1. SEM image of a  $\text{WO}_3$  thin film deposited on  $\text{Si/SiO}_2$  substrate.

Recently, Wang and co-workers reported about a nanocrystalline  $\text{WO}_3$  film deposited by sol–gel that exhibit sub-ppm sensitivity towards  $\text{NO}_2$  at 300 °C [16]. The high surface area offered by mesoporous layers and optimized grain size have been used to obtain a high sensitivity at the operating temperature of 36 °C [17]. Despite that several techniques have been explored to deposit films suitable for gas-sensing applications, less attention has been devoted to thermal evaporation. In this work, a modified thermal evaporation method has been used to deposit nanostructured  $\text{WO}_3$  thin films with high surface roughness and large effective area. Sensing measurements carried out towards  $\text{NO}_2$ ,  $\text{CO}$  and  $\text{NH}_3$  at different temperatures ranging from 100 to 500 °C showed high responses and selectivity towards  $\text{NO}_2$ .

## 2. Experimental

Samples have been deposited by means of a modified thermal evaporation method on 3 mm × 3 mm × 0.25 mm substrates. Alumina ones have been used for the development of sensors while flat silicon ones covered by a thin layer of silicon dioxide have been used for the morphological characterization.

The source material was a metallic tungsten wire with basket shape (SPI Supplies Pk 10 1801). The chamber was evacuated with a rotary pump. The deposition process was carried out in a reactive atmosphere at constant pressure  $p_{\text{O}_2}=0.22$  mbar. A voltage of 5 V was applied to the W basket for 5 min resulting in an electrical current of about 10 A. Substrates were kept 15 mm above the target and heated at the constant temperature of 600 °C. After cooling, the substrates appeared to be covered with a light green film about 1.4  $\mu\text{m}$  thick (measured with an Alphastep profiler).

For comparison,  $\text{WO}_3$  thin films have been deposited on the same substrates by RF magnetron sputtering. The deposition has been performed starting from a metallic target with certified purity at 99.99% in an oxidizing atmosphere with 50% argon and 50% oxygen at a working pressure of  $8 \times 10^{-3}$  mbar. During the deposition process, the substrate was maintained at 300 °C to favour the

formation of a stable layer. The deposition was carried out for 70 min resulting in a 300-nm-thick film. It underwent an annealing cycle at 500 °C for 12 h to enhance the stability of the film during the operation as gas sensor at lower temperatures. Annealing was performed in a furnace under controlled flux of humid synthetic air.

Layers deposited on alumina substrates were provided with interdigitated Pt contacts (IDC) for electrical measurements and with a Pt heater on the backside. Both Pt-structures have been deposited by means of DC magnetron sputtering.

The spacing period of the IDC structure is of 380  $\mu\text{m}$ , with a distance between each “Pt finger” of 190  $\mu\text{m}$ . SEM, TEM and an AFM were used for surface characterization. AFM measurements have been carried out with a Veeco CP-Research microscope in intermittent contact-mode (ic-mode). The tip was a Si one (NT-MDT, NSG10) with a 20-nm diameter and a 22° apex angle. TEM investigation was carried out with FEI Tecnai F20 microscope equipped with field emission source and operated at 200 keV. Bright field imaging has been used for specimen characterization.

The flow-through technique was used to test the gas-sensing properties of the thin films. A constant flux of synthetic air of 0.3 l/min with controlled relative humidity value (RH%) was the gas carrier, into which the desired concentration of pollutants – dispersed in synthetic air – was mixed. All the measurements were executed in a temperature-stabilised sealed chamber with 1 l volume at 20 °C. Electrical characterization was carried out by volt–amperometric technique; the sensor was biased by 1 V and film resistance was measured by a picoammeter, recording data every 20 s.

## 3. Results and discussion

### 3.1. Microstructure characterization

SEM characterization revealed that the film is composed of elongated agglomerates about 500 nm long. The deep holes that separate the elongated agglomerates give the

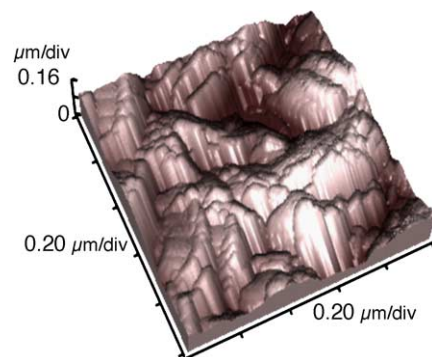


Fig. 2. 1  $\mu\text{m} \times 1 \mu\text{m}$  AFM image of a  $\text{WO}_3$  film deposited on  $\text{Si/SiO}_2$  substrate.

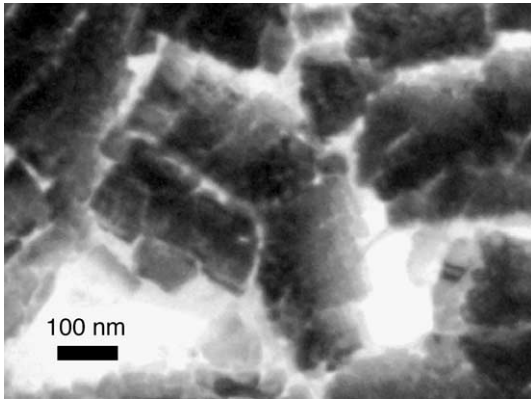


Fig. 3. TEM bright field image of the structure of  $\text{WO}_3$  agglomerate.

sample a mountain like morphology (see Fig. 1). An AFM has been used to obtain three-dimensional characterization of such structures. From  $5 \mu\text{m} \times 5 \mu\text{m}$  AFM images taken in different regions of the sample, the depth of valleys has been estimated to be approximately 200 nm deep, giving an effective area of  $31.4 \mu\text{m}^2$  and a roughness of 49 nm. A  $1 \mu\text{m} \times 1 \mu\text{m}$  zoom image is shown in Fig. 2.

TEM image highlights the structure of the agglomerate as shown in Fig. 3. The agglomerate is composed of particles less than 100 nm in size.

Differently, samples deposited by sputtering exhibit a compact surface as can be noticed from the SEM micrograph reported in Fig. 4.

### 3.2. Sensing characterization

Gas-sensing measurements have been carried out towards  $\text{NO}_2$ ,  $\text{NH}_3$  and  $\text{CO}$  in the temperature range between 100 and 500 °C. Sensors based on thermal evaporated films revealed to be highly sensitive towards  $\text{NO}_2$ , with sensitivity increasing with decreasing working temperature.

The response was calculated as the ratio  $R_{\text{gas}}/R_{\text{air}}$  for oxidizing gases ( $\text{NO}_2$ ) and as  $R_{\text{air}}/R_{\text{gas}}$  for reducing gases ( $\text{CO}$ ,  $\text{NH}_3$ ).  $R_{\text{gas}}$  is the electrical resistance of the film exposed to the target gas and  $R_{\text{air}}$  is the resistance

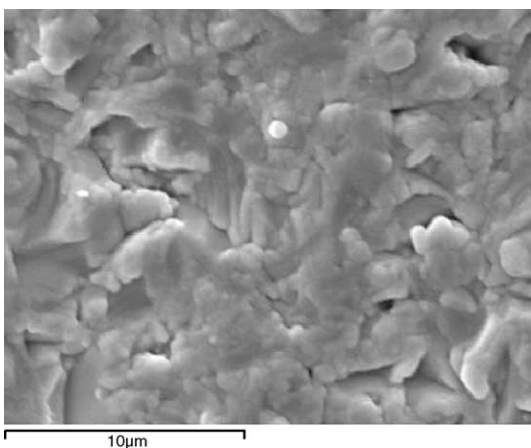


Fig. 4. SEM image of a sputtered  $\text{WO}_3$  film.

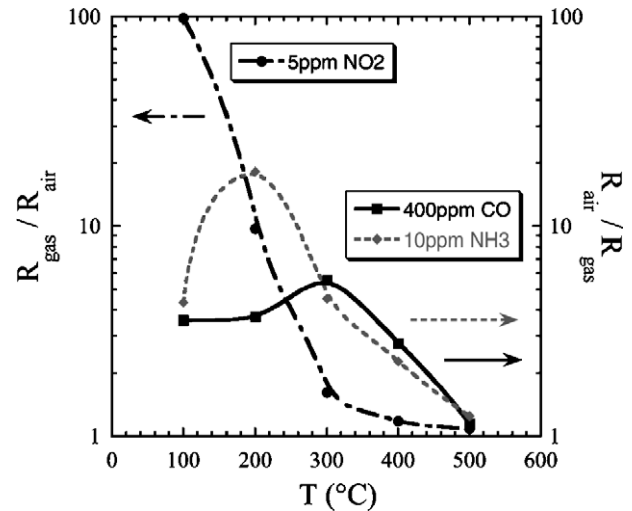


Fig. 5. Temperature dependence of gas responses of  $\text{WO}_3$  films measured for a relative humidity of  $\text{RH}=30\%$ .

measured when the film is exposed to the reference air flux. The temperature dependence of gas response measured at a constant humidity ( $\text{RH}=30\%$ ) is plotted in Fig. 5. Three different regions can be distinguished depending on sensing performances. At temperatures above 300 °C, sensors exhibit low responses towards each tested gas. By decreasing the working temperature, response towards  $\text{NO}_2$  (10 ppm) and  $\text{NH}_3$  (10 ppm) increases and similar values of 12.1 and 18.2 are reached at 200 °C. Response towards  $\text{CO}$  increases up to 300 °C and then start to decrease, but values obtained for the other two gases are never reached.

By lowering the working temperature down to 100 °C, the response to  $\text{NO}_2$  strongly increases while response to  $\text{NH}_3$  has an opposite trend. In this region, the sensors are selective towards  $\text{NO}_2$  against ammonia and  $\text{CO}$ . The responses to sub-ppm  $\text{NO}_2$  concentrations and humidity

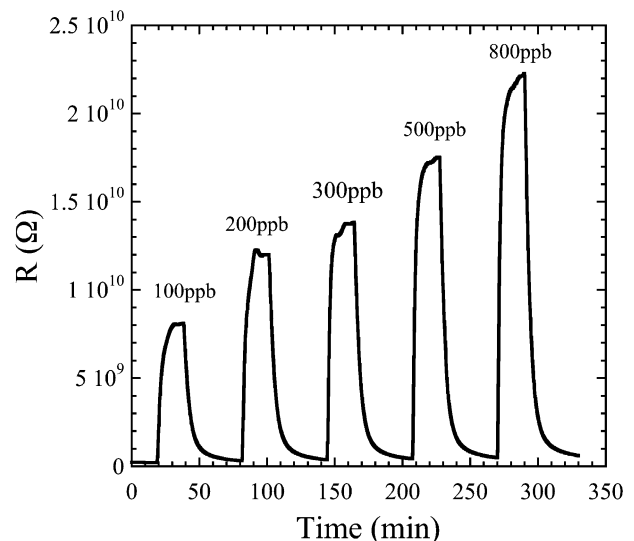


Fig. 6. Responses of  $\text{WO}_3$  films to sub-ppm concentrations of  $\text{NO}_2$  at the operating temperature of 100 °C and relative humidity  $\text{RH}=30\%$ .

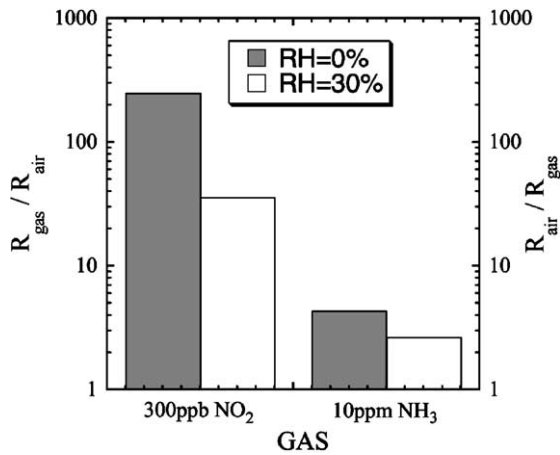


Fig. 7. Humidity effects on responses towards NO<sub>2</sub> and NH<sub>3</sub>. The left y-axis ( $R_{\text{gas}}/R_{\text{air}}$ ) refers to NO<sub>2</sub>-responses, while the right y-axis ( $R_{\text{air}}/R_{\text{gas}}$ ) refers to NH<sub>3</sub>-responses.

effects have also been investigated in this region. Results reported in Fig. 6 highlight that the lower detection limit is less than 100 ppb. Nitrogen dioxide sensing performances are enhanced with decreasing humidity. As shown in Fig. 7 responses towards 300 ppb of NO<sub>2</sub> increase of a factor 7 decreasing the humidity value (RH) from 30 to 0%. The same effect is observed for NH<sub>3</sub> (10 ppm), but with a smaller factor of about 1.5. Results confirm that the selective detection of NO<sub>2</sub> is maintained in dry conditions.

The temperature dependence of the response time ( $\tau_{\text{RISE}}$ ) is plotted in Fig. 8.  $\tau_{\text{RISE}}$  has been calculated as the time the sensor takes to cover the 90% of the difference between the resistance baseline value  $R_{\text{air}}$  and the final value  $R_{\text{gas}}$ .

As the temperature decreases, the response time decreases too, reaching a value of  $160 \pm 20$  s. This is comparable with the chamber filling time, which is about 180 s for the volume of the chamber and the total flux used.

Results in Fig. 8 refer to a concentration of 5 ppm, but a similar trend has been observed for other concentrations

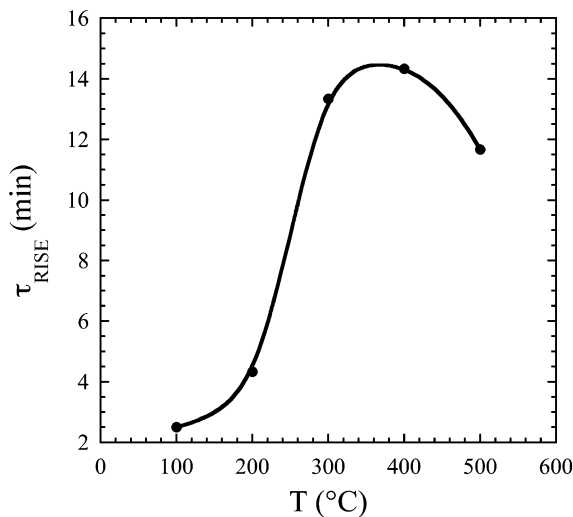


Fig. 8. Temperature dependence of the response time  $\tau_{\text{RISE}}$  of WO<sub>3</sub> films towards 5 ppm of NO<sub>2</sub>, with relative humidity RH=30%.

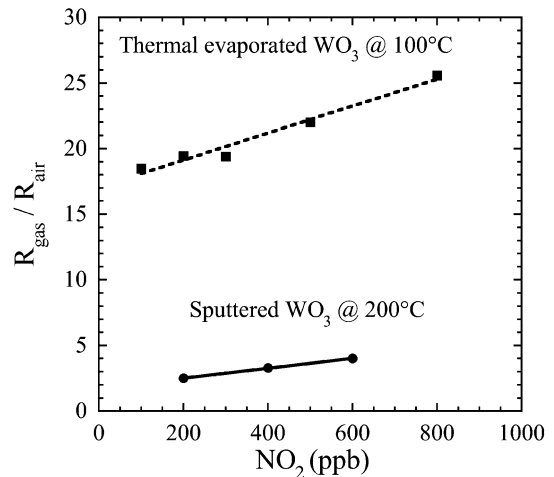


Fig. 9. Comparison between responses to NO<sub>2</sub> obtained from thermal evaporated WO<sub>3</sub> films and from sputtered WO<sub>3</sub> films. All the data are collected using a total flux of 0.3 l/min and RH=30%.

above 1 ppm. The trend cannot be extended to lower concentrations because of the strong reduction occurring in NO<sub>2</sub>-responses with increasing the working temperature (see Fig. 5). Already at 300 °C, responses to sub-ppm concentrations are too small to allow this type of analysis.

The sensing performances of sensors based on evaporated films have been compared to performances exhibited by sputtered ones. In Fig. 9, data measured at the best working temperature, 100 °C for thermal evaporated films and 200 °C for sputtered films, have been reported. Thermal evaporated WO<sub>3</sub> exhibits responses about 5 times higher than the responses obtained from sputtered films. In these experimental conditions, the sensitivity  $S$  has been calculated for both the sensors.  $S$  is defined as the following derivative [18]:

$$S = \partial f / \partial C,$$

where  $f$  is the function relating the response  $r$  of a sensor to the gas concentration  $C$  that caused such a response. In this work,  $r$  has been calculated as the ratio  $R_{\text{gas}}/R_{\text{air}}$  for the NO<sub>2</sub> gas. The sensitivity  $S$  has been locally estimated in the concentration range 100–800 ppb as the linear coefficient resulting from the linear fit applied to data of Fig. 9. Values of  $S=0.010 \text{ ppb}^{-1}$  and  $S=0.004 \text{ ppb}^{-1}$  have been calculated for the thermal evaporated and the sputtered films respectively.

#### 4. Conclusions

The WO<sub>3</sub> thin films based gas sensors were developed by means of fast deposition performed by a reactive thermal evaporation method. Sensors exhibits high responses and selectivity together with low time responses that are enhanced decreasing the working temperature down to the lowest limit of 100 °C, as studied in this work. At this temperature, high sensitivity was reached towards NO<sub>2</sub> with

a detection limit lower than 100 ppb that causes a variation in the film electrical resistance higher than one order of magnitude. This has been proven to be an enhancement with respect to performances obtained with sputtered films. It can be partially ascribed to the high effective area exhibited by thermal evaporated films.

Furthermore, the low responses obtained towards high concentrations of NH<sub>3</sub> (10 ppm) and CO (400 ppm) foresee promising selective properties.

### Acknowledgement

This work has been founded by the European Strep project “Nano-structured solid-state gas sensors with superior performance” (NANOS4) no.: 001528. The authors are grateful to Dr. P. Candeloro for the SEM images.

### References

- [1] K. Bange, T. Gambke, *Adv. Mater.* 2 (1990) 10.
- [2] P.V. Ashrit, G. Bader, Vo-Van Truong, *Thin Solid Films* 320 (1998) 324.
- [3] S.R. Morrison, *The Chemical Physics of Surfaces*, 1st edition, Plenum Press, New York, NY, 1997.
- [4] M.D. Antonik, J.E. Schneider, E.L. Wittman, K. Snow, J.F. Vetelino, R.J. Lad, *Thin Solid Films* 256 (1995) 247.
- [5] N. Yamazoe, *Sens. Actuators, B, Chem.* 5 (1991) 7.
- [6] N.S. Baik, G. Sakai, K. Shimano, N. Miura, N. Yamazoe, *Sens. Actuators, B, Chem.* 65 (2000) 97.
- [7] A.M. Ruiz, G. Sakai, A. Cornet, K. Shimano, J.R. Morante, N. Yamazoe, *Sens. Actuators, B, Chem.* 93 (2003) 509.
- [8] G.S.T. Rao, D.T. Rao, *Sens. Actuators, B, Chem.* 55 (1999) 166.
- [9] C. Cantalini, M.Z. Atashbar, Y. Li, M.K. Ghantasala, S. Santucci, W. Wlodarski, M. Passacantando, *J. Vac. Sci. Technol., A, Vac. Surf. Films* 17 (1999) 1873.
- [10] C. Cantalini, W. Wlodarski, Y. Li, M. Passacantando, S. Santucci, E. Comini, G. Faglia, G. Sberveglieri, *Sens. Actuators, B, Chem.* 64 (2000) 182.
- [11] H. Meixner, J. Gerblinger, U. Lampe, M. Fleisher, *Sens. Actuators, B, Chem.* 23 (1995) 119.
- [12] P.J. Shaver, *Appl. Phys. Lett.* 11 (1967) 255.
- [13] Y.K. Chung, M.H. Kim, W.S. Hum, H.S. Lee, J.K. Song, S.C. Choi, K.M. Yi, M.J. Lee, K.W. Chung, *Sens. Actuators, B, Chem.* 60 (1999) 49.
- [14] G. Sberveglieri, L. Depero, S. Gropelli, P. Nelli, *Sens. Actuators, B, Chem.* 26–27 (1995) 89.
- [15] D. Manno, A. Serra, M. Di Giulio, G. Micocci, A. Tepore, *Thin Solid Films* 324 (1998) 44.
- [16] S.H. Wang, T.C. Chou, C.C. Liu, *Sens. Actuators, B, Chem.* 94 (2003) 343.
- [17] L.G. Teoh, Y.M. Hon, J. Shieh, W.H. Lai, M.H. Hon, *Sens. Actuators, B, Chem.* 96 (2003) 219.
- [18] A. D’Amico, C. Di Natale, *IEEE Sens. J.* 1 (2001) 183.